RESEARCH ARTICLE | OCTOBER 11 2024

Dynamical Casimir effect with screened scalar fields

Special Collection: Quantum Technology and Science in Space

Ana Lucía Báez-Camargo ; Daniel Hartley ; Christian Käding ; Ivette Fuentes

AVS Quantum Sci. 6, 045001 (2024)
https://doi.org/10.1116/5.0222082

Dynamical Casimir effect with screened scalar fields

Cite as: AVS Quantum Sci. 6, 045001 (2024); doi: 10.1116/5.0222082
Submitted: 5 June 2024 · Accepted: 19 September 2024 ·
Published Online: 11 October 2024

Ana Lucía Báez-Camargo,[1,a)] Daniel Hartley,[1] Christian Käding,[2] and Ivette Fuentes[3,b),c)]

AFFILIATIONS

[1]Faculty of Physics, University of Vienna, Boltzmanngasse 5, 1090 Vienna, Austria
[2]Technische Universität Wien, Atominstitut, Stadionallee 2, 1020 Vienna, Austria
[3]School of Physics and Astronomy, University of Southampton, Southampton SO17 1BJ, United Kingdom

Note: This paper is part of the Special Issue on Quantum Technology and Science in Space.
[a)]**Electronic mail:** lucia.baez@univie.ac.at
[b)]**Also at:** Keble College, University of Oxford, Oxford OX1 3PG, United Kingdom.
[c)]Also known as Fuentes-Guridi.

ABSTRACT

Understanding the nature of dark energy and dark matter is one of modern physics' greatest open problems. Scalar-tensor theories with screened scalar fields like the chameleon model are among the most popular proposed solutions. In this article, we present the first analysis of the impact of a chameleon field on the dynamical Casimir effect, whose main feature is the particle production associated with a resonant condition of boundary periodic motion in cavities. For this, we employ a recently developed method to compute the evolution of confined quantum scalar fields in a globally hyperbolic spacetime by means of time-dependent Bogoliubov transformations. As a result, we show that particle production is reduced due to the presence of the chameleon field. In addition, our results for the Bogoliubov coefficients and the mean number of created particles agree with known results in the absence of a chameleon field. Our results initiate the discussion of the evolution of quantum fields on screened scalar field backgrounds.

I. INTRODUCTION

Quantum field theory in curved spacetime (QFTCS) studies the behavior of quantum fields propagating in a classical relativistic background geometry.[1–3] This theory has predicted many physical phenomena, such as cosmological particle creation,[3–5] Hawking radiation,[6] and the Unruh effect,[7] as well as the dynamical Casimir effect (DCE),[8] which refers to the generation of particles due to the motion of boundaries (see Refs. 9–11 for reviews). The first computations of the DCE were done in flat spacetime.[8,12] Over the past five decades, numerous developments have appeared including distinct geometries of the cavities,[13–15] entanglement generation,[16–19] and extensions to a few other metrics.[20,21] Performing a mathematically rigorous study of the DCE is challenging due to the complexity of studying quantum field theory with dynamical boundary conditions.[22,23] For this reason, within the framework of QFTCS, in Refs. 24 and 25, some of the authors of the present work introduced a general method to compute the evolution of a confined quantum scalar field in a globally hyperbolic spacetime by means of a time-dependent Bogoliubov transformation. Part I[24] considers spacetimes without boundaries or with timelike boundaries that remain static in some synchronous frame, while Part II[25] considers spacetimes with timelike boundaries that do not remain static in any synchronous frame.

QFTCS builds on the framework of general relativity (GR), which has proven to be a remarkably successful theory of gravity and cosmology.[26,27] Many physical predictions of GR have been experimentally validated over the last century, the most recent being the detection of gravitational waves.[28] However, GR has some well-known limitations, such as the breakdown of the equivalence principle at singularities, or the accelerating expansion of the Universe and the mystery of dark energy (responsible for this accelerated expansion). Therefore, many different modifications to GR have been proposed. Among these modified theories of gravity, scalar-tensor theories[29] are some of the most studied. There are two major reasons to study such theories; first, it is one of the simplest ways to modify GR, and second, some extensions of the standard model of particle physics predict the existence of scalar fields.[30,31] This is further motivated by the experimentally confirmed existence of

one scalar field in Nature, namely, the Higgs field.[32–34] Moreover, there are several proposed explanations for the nature of dark energy based on scalar-tensor theories.[35,36] Some of these models predict a fifth force, which has not yet been detected on Earth or in the Solar System.[37–39]

One way to mitigate this tension between theory and observation is by introducing a "screening mechanism,"[40] which allows the effects of the additional scalar fields to vary depending on the environment. Therefore, a screening mechanism would enable additional scalar fields to contribute to dark energy or dark matter while evading current experimental constraints on fifth forces. There are several models for such screened scalar fields with different types of screening mechanisms, such as chameleons;[41,42] symmetrons,[43–50] whose fifth forces have been suggested as alternatives to particle dark matter;[51–54] galileons;[55–57] and environment-dependent dilatons.[45,58–62] Most of these models have been or are proposed to be tested in a zoo of different experiments and observations, for example, Refs. 40 and 63–89. Furthermore, in recent years, there have been initial attempts to study screened scalars as quantum fields,[90–93] and it was proposed to study screened scalar-tensor theories in analog gravity simulations.[94]

Additional proposals in the particular case of chameleon fields suggest that experiments which measure Casimir forces may also be used to constrain chameleon theories.[95–102] From a theoretical point of view, a natural extension of the previous proposals then arises: if the chameleon field can be constrained by the static Casimir effect, then it might also be constrained by the dynamical Casimir effect. Thus, the aim of the present work is to study the DCE in the presence of a chameleon field, and to explore the relationship between the particle production and the chameleon field parameters. As a first step toward estimating the feasibility of constraining chameleon fields with the DCE, we consider a toy model with only the effect of the chameleon field and no gravity. Since the problem we want to solve in this work is that of a confined quantum field with moving boundaries, we will use the techniques developed in Ref. 25.

This paper is organized as follows: In Sec. II A, we introduce screened scalar fields using the example of the chameleon mechanism; and, in Sec. II B, we describe some relevant aspects of QFTCS applied to the DCE and, in particular, the method developed in Ref. 25. Section III is the nuclear part of the article, where we obtain the main result, and analyze it both analytically and with a numerical example. We conclude in Sec. IV. In addition, in Appendix A, we show the derivation of the normalization constant of the cavity modes. We use natural units $\hbar = c = 1$ throughout the article.

II. BACKGROUND

In this section, we give an overview of scalar-tensor theories of gravitation, in particular screened scalar fields and the chameleon model. In addition, we show schematically the usual approach to studying the DCE within the framework of QFTCS, and we then outline the techniques that are used in the present work.

A. Screened scalar fields

The aim of scalar-tensor theories of gravitation is to study the modifications of GR due to an additional scalar field which is coupled to the metric tensor. A common way of performing such a coupling between a scalar field φ and the metric tensor $g_{\mu\nu}$ is through a conformal factor $A^2(\varphi)$, such that

$$\tilde{g}_{\mu\nu} = A^2(\varphi) g_{\mu\nu}. \tag{1}$$

In this sense, scalar-tensor theories of gravity are defined up to a conformal transformation leading from one so-called conformal frame to another.[103] These conformal frames are merely different mathematical formulations. Hence, the theoretical prediction for an observable quantity cannot be altered due to a change of conformal frame. The advantage is that some calculations might be easier to perform in one frame than in another. Two popular conformal frames are the Jordan frame—with a metric we denote $\tilde{g}_{\mu\nu}$—and the Einstein frame denoted as $g_{\mu\nu}$.

Even though the physical measurement cannot be changed, the physical interpretation can actually differ from one frame to another.[104] For example, in the Jordan frame formulation, Einstein's theory of gravity is modified in such a way that test particles follow different geodesics from those predicted in GR, while in the Einstein frame formulation, test particles still follow GR's geodesics but are also subject to a gravity-like fifth force of Nature carried by the additional scalar field φ. The problem with such a prediction is that fifth forces are tightly constrained in our Solar System. An interesting way to solve this issue is given by so-called screening mechanisms. Such a mechanism allows the fifth force to be weak within our Solar System but cosmologically significant on intergalactic scales. As we describe in the Introduction, Sec. I, there are several models for such screened scalar fields with different types of screening mechanisms such as the chameleon model, which will be presented in more detail in Sec. II A 2.

1. Einstein-frame action

In this article, we consider a universe containing a free scalar field Φ, which we denote as the "matter," with mass m_Φ; and an additional scalar field φ conformally coupling to the metric tensor. In the Einstein frame, this universe's action is schematically given by

$$S_{Universe} = S_{gravity} + S_m + S_\varphi, \tag{2}$$

where $S_{gravity}$ is the usual Einstein–Hilbert gravitational action, S_m is the matter action, and S_φ is the action of the scalar field φ. Following Ref. 91, the conformal coupling to the metric tensor induces an interaction between Φ and φ, which in turn leads to a rescaling of the free field's mass by the conformal factor. More precisely, Ref. 91 starts with a free Jordan frame scalar field $\tilde{\Phi}$ described by the Jordan frame Lagrangian $\tilde{\mathcal{L}}_m$, translates both into the Einstein frame via $\Phi = A(\varphi)\tilde{\Phi}$ and $\mathcal{L}_m = A^4(\varphi)\tilde{\mathcal{L}}_m$, and then, using that the conformal factor is an analytic function of φ, keeps only operators up to dimension four. Consequently, the Lagrangian matter density associated with the action S_m is given by

$$\mathcal{L}_m = -\frac{1}{2} g^{\mu\nu} \partial_\mu \Phi \partial_\nu \Phi - \frac{1}{2} A^2(\varphi) m_\Phi^2 \Phi^2. \tag{3}$$

Subsequently, from the Euler–Lagrange equations, we obtain the equation of motion for the probe field Φ:

$$g^{\mu\nu} \partial_\mu \partial_\nu \Phi - A^2(\varphi) m_\Phi^2 \Phi = 0. \tag{4}$$

Later, in Sec. III, we will ignore gravity for simplicity and consequently set $g_{\mu\nu} = \eta_{\mu\nu}$.

2. Chameleon model

A chameleon scalar field model has the defining property of coupling to matter in such a way that its effective mass increases with increasing local matter density. As its name suggests, the chameleon

field adapts to its environment and becomes almost impossible to detect in regions of high matter density like our Solar System. The conformal coupling factor in Eq. (1) of a chameleon is given by

$$A^2(\varphi) = e^{2\varphi/M}, \tag{5}$$

where M is a mass scale which determines the strength of the chameleon-matter coupling. As is common practice when dealing with chameleons, we assume that $\varphi/M \ll 1$. The Lagrangian density describing the chameleon field and associated with the action S_φ in Eq. (2) is

$$\mathcal{L}_\varphi = -\frac{1}{2}(\partial\varphi)^2 - \frac{\Lambda^{4+N}}{\varphi^N} - \frac{\varphi}{M}\rho, \tag{6}$$

where $N \in \mathbb{Z}^+ \cup 2\mathbb{Z}^- \backslash \{-2\}$ distinguishes between different chameleon models; the parameter Λ determines the strength of the self-interaction; and ρ is the density of non-relativistic matter that the chameleon is interacting with. It should be noted that, in the case $N = -4$, the self-interaction term in Eq. (6) is actually given by $\lambda\varphi^4/4!$ with a dimensionless constant λ. The sum of the last two terms in Eq. (6) results in an effective potential with a local minimum, and consequently a non-vanishing chameleon mass which increases with the matter density. Since the chameleon fifth force usually has a Yukawa-like suppression,[41] its range is the shorter the larger the chameleon's mass. Consequently, in environments of sufficiently high density, the chameleon fifth force is effectively quite feeble, i.e., screened.

Consider a static spherically symmetric source of radius R and homogeneous density ρ_{obj} immersed in a homogeneous medium of density ρ_{bg}. The field profile outside of this source, but still within an ambient Compton wavelength ($r < m_{bg}^{-1}$) with m_{bg} being the chameleon's mass in the medium of density ρ_{bg}, is approximately given by[71]

$$\varphi \simeq \varphi_{bg} - \frac{R}{r}(\varphi_{bg} - \varphi_{obj}), \tag{7}$$

where φ_{obj} is the value of the chameleon field inside the source and φ_{bg} is the value of the chameleon field outside the source or the so-called background value. In the case of a large density contrast $\rho_{obj} \gg \rho_{bg}$, we can consider $\varphi_{bg} \gg \varphi_{obj}$. If the source is screened, then φ_{obj} is actually the minimum of the chameleon within the source apart from a thin shell near the surface. Only the matter in this thin shell sources the chameleon fifth force in the exterior while the interior is not contributing. This is due to the short range of the fifth force in case of a large effective chameleon mass, and is known as the *thin-shell effect*. In order to know if the chameleon field is screened or not, we define the shell thickness

$$\Delta R = \frac{M\varphi_{bg}}{\rho_{obj}R}. \tag{8}$$

The object is said to be screened if $\Delta R \ll R$ or

$$\frac{M\varphi_{bg}}{\rho_{obj}R^2} \ll 1. \tag{9}$$

B. Dynamical Casimir effect, quantum field theory, and particle content

The usual approach to studying the DCE is to consider a free scalar field Φ in a one-dimensional[105] cavity with perfectly reflecting boundaries satisfying the Klein–Gordon equation,

$$g^{\mu\nu}\nabla_\mu\nabla_\nu\Phi - m_\Phi^2\Phi - \xi\mathcal{R}\Phi = 0, \tag{10}$$

where $m_\Phi \geq 0$ is the rest mass of the field, $g^{\mu\nu}$ is the spacetime metric, $\mathcal{R}$ its scalar curvature, and $\xi \in \mathbb{R}$ is a coupling constant. Let us consider flat spacetime in inertial coordinates (t, x). The boundaries of the cavity are moved during the time $t_0 < t < t_f$. Since we are considering ideally reflecting boundaries, we impose Dirichlet vanishing boundary conditions,

$$\Phi(t, x = x_l(t)) = \Phi(t, x = x_r(t)) = 0, \tag{11}$$

where the functions $x_l(t)$ and $x_r(t)$ determine the positions of the left and right boundaries for $t_0 < t < t_f$, respectively. Before the boundaries move ($t < t_0$), we assume that the walls are static. For such initial conditions, the quantized field operator is decomposed as follows:[1]

$$\hat{\Phi}(t, x) = \sum_n \left[\hat{a}_n\phi_n(t, x) + \hat{a}_n^\dagger\phi_n^*(t, x)\right], \tag{12}$$

where the mode functions $\phi_n(t, x)$ are solutions to the Klein–Gordon equation (10). In addition, $\hat{a}_n$ and $\hat{a}_n^\dagger$ are the bosonic annihilation and creation operators, respectively. Hence, the Fock space and vacuum state are defined in the canonical way. Two sets of mode solutions are related by a Bogoliubov transformation. In this way, the effects of the moving boundaries on the quantum field can be computed using a Bogoliubov transformation,[1] such that

$$\begin{aligned} \tilde{\phi}_m &= \sum_n \left[\alpha_{mn}\phi_n + \beta_{mn}\phi_n^*\right], \\ \tilde{a}_m &= \sum_n \left[\alpha_{mn}^*\hat{a}_n - \beta_{mn}^*\hat{a}_n^\dagger\right], \end{aligned} \tag{13}$$

where α_{mn} and β_{mn} are called Bogoliubov coefficients. Note that if $\beta_{mn} \neq 0$, then the transformation of the annihilation operator of Eq. (13) contains creation operators. Therefore, the two vacua do not coincide. Hence, the β-coefficients quantify particle creation due to the transformation. Starting with a vacuum state, the average number of particles in mode m after a Bogoliubov transformation is given by

$$\mathcal{N}_m = \sum_n |\beta_{nm}|^2. \tag{14}$$

In general, the computation of the Bogoliubov coefficients is difficult. Thus, mathematical techniques and simplifications adapted to a specific problem make the computations manageable. For instance, the presence of symmetries like homogeneity or isotropy is convenient to obtain results on particle creation in cosmological models. In Refs. 24 and 25, the authors developed a method to compute the Bogoliubov transformation experienced by a confined quantum scalar field in a globally hyperbolic spacetime due to the changes in the geometry and/or the confining boundaries. The second part[25] extends the method to cases in which the timelike boundaries of the spacetime do not remain static in any synchronous frame. This method is especially useful in the presence of resonances of the field modes due to small perturbations of the metric and/or the motion of the cavity boundaries. This is because in these cases, the Bogoliubov coefficients take the following simple expressions:

$$\begin{aligned} &\alpha_{nn}(t_f, t_0) \approx 1, \\ &\alpha_{nm}(t_f, t_0) \approx \varepsilon \int_{t_0}^{t_f} dt\, e^{-i(\omega_n^0 - \omega_m^0)t}\Delta\hat{\alpha}_{nm}(t), \quad n \neq m, \end{aligned} \tag{15}$$

$$\beta_{nm}(t_f,t_0) \approx \varepsilon \int_{t_0}^{t_f} \mathrm{d}t\, \mathrm{e}^{-\mathrm{i}(\omega_n^0+\omega_m^0)t} \Delta\hat{\beta}_{nm}(t), \tag{16}$$

where $\varepsilon \ll 1$ is a small parameter that characterizes the perturbation of the confined field (e.g., oscillation amplitude), and ω_n^0 are the mode frequencies for the static problem ($\varepsilon = 0$). For Dirichlet boundary conditions,

$$\begin{aligned}\Delta\hat{\alpha}_{nm}(t) \equiv\ & \mathrm{i}\int_{\Sigma^0} \mathrm{d}V^0 \left[{}^{-}_{m}\hat{\Delta}(t)\Psi_n^0\right]\Psi_m^0 \\ & - \mathrm{i}\int_{\partial\Sigma_0} \mathrm{d}S^0\, \Delta x(t)\left(\mathbf{n}\cdot\nabla_{h^0}\Psi_n^0\right)\left(\mathbf{n}\cdot\nabla_{h^0}\Psi_m^0\right), \end{aligned}\tag{17}$$

$$\begin{aligned}\Delta\hat{\beta}_{nm}(t) \equiv\ & -\mathrm{i}\int_{\Sigma^0} \mathrm{d}V^0 \left[{}^{+}_{m}\hat{\Delta}(t)\Psi_n^0\right]\Psi_m^0 \\ & + \mathrm{i}\int_{\partial\Sigma_0} \mathrm{d}S^0\, \Delta x(t)\left(\mathbf{n}\cdot\nabla_{h^0}\Psi_n^0\right)\left(\mathbf{n}\cdot\nabla_{h^0}\Psi_m^0\right). \end{aligned}\tag{18}$$

Here, Σ^0 is a fixed spatial hypersurface, around which the perturbation occurs, with volume element dV^0; boundary $\partial\Sigma^0$; boundary surface element dS^0; proper distance $\varepsilon\Delta x(t)$ between the boundary $\partial\Sigma_t$ and the fixed boundary $\partial\Sigma^0$; and connection ∇_{h^0} associated with the static metric h_{ij}^0. ${}^{\pm}_{m}\hat{\Delta}(t)$ are linear operators determined by their actions on the mode basis $\{\Psi_n^0\}$ as defined in Eq. (50) of Ref. 25.

The Bogoliubov transformation differs maximally from the identity just by terms of first order in ε, except for the cases where there are resonances. If the perturbation considered contains some characteristic frequency ω_p, such that it coincides with some difference between the frequencies of two modes, $\omega_p = \omega_n^0 - \omega_m^0$, then the corresponding coefficient $\alpha_{nm}(t_f,t_0)$ grows linearly with the time difference $t_f - t_0$ and eventually grows to be a non-perturbative correction. Respectively, if the characteristic frequency coincides with some sum between the frequencies of two modes, $\omega_p = \omega_n^0 + \omega_m^0$, then the coefficient $\beta_{nm}(t_f,t_0)$ grows linearly in time. The duration of the perturbation Δt should be such that $1 \ll \omega_p \Delta t \ll 1/\varepsilon$. This is because the period of time should be reasonably larger than the inverse of the frequency being described, but on the other hand, one should keep higher order terms in ε significantly smaller than the first order term to ensure the validity of the perturbative computation.

III. DYNAMICAL CASIMIR EFFECT IN A SPACETIME WITH A SCREENED SCALAR FIELD

In this section, we study the toy model of a DCE for a minimally coupled massive quantum scalar field in a spacetime affected by a chameleon field $\varphi = \varphi(\mathbf{x})$. Let us consider the spacetime metric to be the Minkowski metric $\eta_{\mu\nu}$ and a quantum field trapped inside an effectively one-dimensional cavity[106] of average proper length L. The cavity is placed at a distance d to a sphere of radius R, which acts as a source for the chameleon force. We consider coordinates centered on the sphere, where x is the radial distance to the center of the sphere. The boundaries of the cavity are placed at x_l (left) and x_r (right), and the right boundary oscillates with frequency Ω and amplitude $\varepsilon L \ll L$, such that the cavity is oscillating as

$$x_l = s, \quad x_r(t) = s + L[1 + \varepsilon\sin(\Omega t)], \tag{19}$$

where $s = R + d$. We impose Dirichlet boundary conditions on the scalar field at the boundaries and ignore the gravitational field of the chameleon source mass. This toy model will help us to understand the qualitative behavior of a confined quantum field with moving boundaries in a spacetime with a screened scalar field.

Since the Minkowski metric $\eta_{\mu\nu}$ is a synchronous frame, we can use the method displayed in Ref. 25 right away. Focusing on the small perturbations regime for the problem under consideration, the quantities needed to compute Eqs. (17) and (18) are

$${}^{\pm}_{m}\hat{\Delta} = 0, \tag{20}$$

$$\Delta x(s) = 0, \quad \Delta x(s+L) = L\sin(\Omega t). \tag{21}$$

Using Eq. (4), the static spatial eigenvalue equation (34) of Ref. 25 and the boundary conditions read

$$\begin{aligned}&\partial_x^2\Psi_n^0 + \left[(\omega_n^0)^2 - A^2(\varphi)m_\Phi^2\right]\Psi_n^0 = 0, \\ &\Psi_n^0(x_l = s) = \Psi_n^0(x_r(0) = s+L) = 0.\end{aligned}\tag{22}$$

A. Solution to the static eigenvalue equation

Since we have assumed $\varphi/M \ll 1$, see Sec. II A 2, the chameleon coupling function in Eq. (5) can be approximated by

$$A^2(\varphi) = 1 + 2\frac{\varphi(x)}{M} + \mathcal{O}\left(\frac{\varphi^2}{M^2}\right). \tag{23}$$

The chameleon profile given in Eq. (7) is a function of $1/r$ with $r > 0$. Thus, assuming that the cavity is sufficiently far from the source mass center, i.e., $L \ll s$, it is possible to linearize the field profile within the cavity $x \in [x_l, x_r]$, such that

$$\varphi(x) \approx \varphi_{bg} - 2\varphi_{bg}\frac{R}{s} + \varphi_{bg}\frac{R}{s^2}x. \tag{24}$$

Substituting Eq. (24) in the eigenvalue equation (22), we have

$$\begin{aligned}&\partial_x^2\Psi_n^0 - 2\frac{\varphi_{bg}}{M}\frac{R}{s^2}xm_\Phi^2\Psi_n^0 \\ &\quad + \left[(\omega_n^0)^2 - \left[1 + 2\frac{\varphi_{bg}}{M} - 4\frac{\varphi_{bg}}{M}\frac{R}{s}\right]m_\Phi^2\right]\Psi_n^0 = 0.\end{aligned}\tag{25}$$

Following the technique presented in Ref. 107, we define the quantities

$$a := 2\frac{\varphi_{bg}}{M}\frac{R}{s^2}m_\Phi^2, \tag{26}$$

$$b := 1 + 2\frac{\varphi_{bg}}{M} - 4\frac{\varphi_{bg}}{M}\frac{R}{s}, \tag{27}$$

$$\lambda_n^2 := (\omega_n^0)^2 - bm_\Phi^2. \tag{28}$$

Furthermore, we introduce a new variable,

$$u := u_n(x) = \left(\frac{\lambda_n^2}{a} - x\right)(a)^{1/3}. \tag{29}$$

From here on, we omit the explicit dependence of u on n for simplicity in the notation. Then the eigenvalue equation (25) can be rewritten as

$$\partial_u^2\Psi_n^0 + u\Psi_n^0 = 0, \tag{30}$$

which is an Airy differential equation. The solution of Eq. (30) is given by means of Bessel functions,

$$\Psi_n^0(u) = \sqrt{u}\left[c_1 J_{1/3}\left(\frac{2}{3}u^{3/2}\right) + c_2 J_{-1/3}\left(\frac{2}{3}u^{3/2}\right)\right]. \tag{31}$$

To progress further in this derivation, we must assume that $u \gg 1$. Therefore, we can apply the asymptotic form of Eq. (31) as seen in Ref. 107, such that

$$\Psi_n^0(u) = \mathcal{A}_n u^{-1/4} \sin\left(\frac{2}{3}u^{3/2} + \phi\right) \tag{32}$$

with $\mathcal{A}_n$ and ϕ being constants. While $u \gg 1$ is not globally true, we show in Sec. III C that the region of the parameter space of the considered chameleon models, for which this assumption can be applied, is largely unconstrained by experiments.

To guarantee that the field satisfies the Dirichlet boundary conditions, we require that

$$\frac{2}{3}\left[u^{3/2}(x_r) - u^{3/2}(x_l)\right] = n\pi, \quad n \in \mathbb{N}. \tag{33}$$

The next approximation we make is that the variation of u within the cavity is small. This lets us linearize $[u(x)]^{3/2}$ at the point s,

$$[u(x)]^{3/2} \approx [u(s)]^{1/2}\left[u(s) + \frac{3}{2}[u'(s)](x-s)\right]. \tag{34}$$

Then Eq. (33) becomes

$$[u(s)]^{1/2}u'(s)L = n\pi. \tag{35}$$

Substituting Eqs. (29) and (28) in Eq. (35), we obtain

$$(\omega_n^0)^2 = k_n^2 + m_\Phi^2\left(1 + 2\frac{\varphi_{bg}}{M}\left[1 - \frac{R}{s}\right]\right), \tag{36}$$

where $k_n = \frac{n\pi}{L}$. Note that if the chameleon field is turned off, we recover the usual frequencies of the static problem in flat spacetime for a massive field,[1]

$$\omega_{n_f}^0 = \sqrt{k_n^2 + m_\Phi^2}. \tag{37}$$

From Eq. (32) and the boundary condition $\Psi_n^0(x_l) = 0$, we see that

$$\phi = -\frac{2}{3}u^{3/2}(x_l). \tag{38}$$

Applying the normalization condition given in Eq. (36) of Ref. 25, we obtain

$$\mathcal{A}_n = \left[2\omega_n^0\int_{x_l}^{x_r} dx\, u^{-1/2}(x)\sin^2\left(\frac{2}{3}u^{3/2}(x) - \frac{2}{3}u^{3/2}(x_l)\right)\right]^{-1/2}. \tag{39}$$

Using Eq. (34) and doing another linearization of $u^{-1/2}(x)$ at the point s, we obtain after some algebra,

$$\mathcal{A}_n = \frac{2(k_n^2)^{3/4}}{(\omega_n^0 L)^{1/2}(a)^{1/6}(4k_n^2 + aL)^{1/2}}. \tag{40}$$

The full derivation of this normalization constant can be found in the Appendix.

B. Bogoliubov coefficients

In order to compute the Bogoliubov coefficients in Eqs. (15) and (16), we first need to compute the quantities in Eqs. (17) and (18). Note that the first integrals of Eqs. (17) and (18) vanish since the operator $\frac{\pm}{m}\hat{\Delta}$ is zero [as seen in Eq. (20)]. For the second integrals, we substitute Eq. (21). Since we are considering one spatial dimension, the "surface integral" is simply the evaluation of the integrand at the two static boundaries, such that

$$\begin{aligned}\Delta\hat{\alpha}_{nl} &= -iL\sin(\Omega t)(-1)^{n+l}\mathcal{A}_n\mathcal{A}_l(a)^{1/3}\left[\left(\lambda_n^2 - ax_r\right)\left(\lambda_l^2 - ax_r\right)\right]^{1/4} \\ &= -\Delta\hat{\beta}_{nl}.\end{aligned} \tag{41}$$

Substituting Eq. (40) in Eq. (41) and considering that the oscillation frequency of the boundary coincides with the difference of the mode frequencies, that is $\Omega = |\omega_n^0 - \omega_l^0|$, then we see that the α-coefficients from Eq. (15) are given by

$$\begin{aligned}&\alpha_{nl}(t_f, t_0) \\ &\approx -\varepsilon\frac{2(-1)^{n+l}(t_f - t_0)}{(\omega_n^0\omega_l^0)^{1/2}}\frac{\left[k_n^2k_l^2\right]^{3/4}\left[k_n^2k_l^2 - aL\left(k_n^2 + k_l^2\right) + a^2L^2\right]^{1/4}}{\left[16k_n^2k_l^2 + aL\left(4k_n^2 + 4k_l^2\right) + a^2L^2\right]^{1/2}}.\end{aligned} \tag{42}$$

If, instead, the oscillation frequency of the boundary coincides with the sum of the mode frequencies, that is $\Omega = \omega_n^0 + \omega_l^0$, then Eq. (16) is

$$\begin{aligned}&\beta_{nl}(t_f, t_0) \\ &\approx \varepsilon\frac{2(-1)^{n+l}(t_f - t_0)}{(\omega_n^0\omega_l^0)^{1/2}}\frac{\left[k_n^2k_l^2\right]^{3/4}\left[k_n^2k_l^2 - aL\left(k_n^2 + k_l^2\right) + a^2L^2\right]^{1/4}}{\left[16k_n^2k_l^2 + aL\left(4k_n^2 + 4k_l^2\right) + a^2L^2\right]^{1/2}}.\end{aligned} \tag{43}$$

Equations (42) and (43) are the general results of this work. Recall that these coefficients are obtained in the presence of resonances where the corresponding coefficient grows linearly with time. Hence, after enough time the effect becomes significant and non-perturbative.

C. Analysis

If we expand Eq. (43) around the small parameter $\frac{\varphi_{bg}}{M}$ up to first order [since the second order is negligible, see Eq. (23)], we obtain

$$\beta_{nl}(t_f, t_0) \approx \frac{(-1)^{n+l}\varepsilon k_n k_l(t_f - t_0)}{2\left(\omega_{n_f}^0\omega_{l_f}^0\right)^{1/2}}\left\{1 - B_{nl} + \mathcal{O}\left(\frac{\varphi_{bg}^2}{M^2}\right)\right\}. \tag{44}$$

We see that the zeroth order approximation, when the chameleon field is turned off, gives the usual coefficients of the DCE in Minkowski spacetime.[25,108,109] Thus, the zeroth order approximation exhibits the familiar resonance behavior in the β-coefficients. The first order approximation is given by

$$\begin{aligned}B_{nl} = \frac{m_\Phi^2}{2}\frac{\varphi_{bg}}{M}\Bigg[&\left(\frac{1}{\left[\omega_{n_f}^0\right]^2} + \frac{1}{\left[\omega_{l_f}^0\right]^2}\right) - \frac{R}{s}\left(\frac{1}{\left[\omega_{n_f}^0\right]^2} + \frac{1}{\left[\omega_{l_f}^0\right]^2}\right) \\ &+ \frac{3}{2}\frac{RL}{s^2}\left(\frac{k_n^2 + k_l^2}{k_n^2k_l^2}\right)\Bigg].\end{aligned} \tag{45}$$

Equation (45) gives a novel contribution due to the chameleon field, where the first term is a constant independent of the geometry. The second contribution depends on the position of the cavity in relation

TABLE I. Parameters used to compute the chameleon contribution to the particle content of the confined quantum field.

Parameter	Symbol	Value
Cavity length	L	$50\,\mathrm{eV}^{-1}$ ($\sim 10^{-5}$ m)
Cavity field mass	m_Φ	497×10^6 eV (mass of kaon K^0)
Source mass radius	R	$1000\,\mathrm{eV}^{-1}$ (2×10^{-4} m)
Distance from center of source mass to cavity	s	$5000\,\mathrm{eV}^{-1}$ ($\sim 10^{-3}$ m)
Vacuum chamber radius	R_{vac}	$2.5 \times 10^5\,\mathrm{eV}^{-1}$ (5×10^{-2} m)

to the chameleon source, while the third term depends on the length of the cavity and tells us about the strength of the chameleon gradient between the two ends of the cavity, reminiscent of the structure of a linearized Newtonian gravitational potential. Since we are already in the resonance regime $\Omega = \omega_n^0 + \omega_l^0$, the sum in the number of particles in Eq. (14) disappears, such that the average particle number is given by

$$|\beta_{nl}(t_f, t_0)|^2 \approx \frac{\varepsilon^2 k_n^2 k_l^2 (t_f - t_0)^2}{4\left(\omega_{n_f}^0 \omega_{l_f}^0\right)}\{1 - 2B_{nl}\}. \tag{46}$$

To see how the chameleon contribution affects the β-coefficients and thus the particle number, let us consider that the cavity and the chameleon source are inside a vacuum chamber of radius R_{vac}. We plot the contours for B_{nl} using the parameters shown in Table I. Note that we consider a kaon K^0 as the massive quantum scalar field in our toy model.

In order to obtain the chameleon background value, we use the relation given in Refs. 68 and 71,

$$\varphi_{bg}(\Lambda) = \xi\left(N(N+1)\Lambda^{4+N} R_{vac}^2\right)^{1/N+2}, \tag{47}$$

where ξ is a "fudge factor" largely insensitive to N, Λ, and M, as well as to the assumed chamber geometry. Here, we assume the conservative value of $\xi = 0.55$.[71] We consider the chameleon models $N = 1$ and $N = -4$, which are the most studied ones.[40] For the chameleon model with $N = -4$, the Lagrangian in Eq. (6) changes to

$$\mathcal{L} = -\frac{1}{2}(\partial\varphi)^2 - \frac{\lambda}{4!}\varphi^4 - \frac{\varphi}{\mathcal{M}}\rho. \tag{48}$$

Hence, in this case, Eq. (47) is given by

$$\varphi_{bg} = \xi\sqrt{\frac{2}{\lambda}\frac{1}{R}}, \tag{49}$$

where $\lambda = (\Lambda/\Lambda_{DE})^4$ and $\Lambda_{DE} = 2.4$ meV is the dark energy scale.[40]

Figure 1 shows the chameleon contribution to the Bogoliubov coefficients and consequently to the particle number for the chameleon model $N = 1$, where, more precisely, Fig. 1(a) depicts the chameleon contribution as a function of Λ and M. The parameter M is essentially unconstrained but probably below the reduced Planck mass $M_{Pl} \approx 2.4 \times 10^{18}$ GeV.[68] Here, we use a subset of the parameter spaces shown in Refs. 81 and 85, where the assumption made in Eq. (29) is fulfilled, namely $u \gg 1$.[110] Figure 1(b) shows the chameleon contribution as a function of the cavity mode number n. Note that the chameleon contribution is stronger for the upper left corner in Fig. 1(a). In addition, also note that, for fixed Λ and M, the chameleon contribution is the strongest for the quantum number $n = 1$, but decays with increasing n.

Furthermore, in Fig. 2, we present the chameleon contribution to the Bogoliubov coefficients and consequently to the particle number for the chameleon model $N = -4$. Figure 2(a) shows the chameleon contribution as a function of Λ and M, and Fig. 2(b) depicts it as a function of the cavity mode number n. Note that, in contrast to Fig. 1(a), the chameleon contribution is stronger in the lower left corner in Fig. 2(a), while, for fixed Λ and M, it behaves in the same way as it did for the chameleon model $N = 1$.

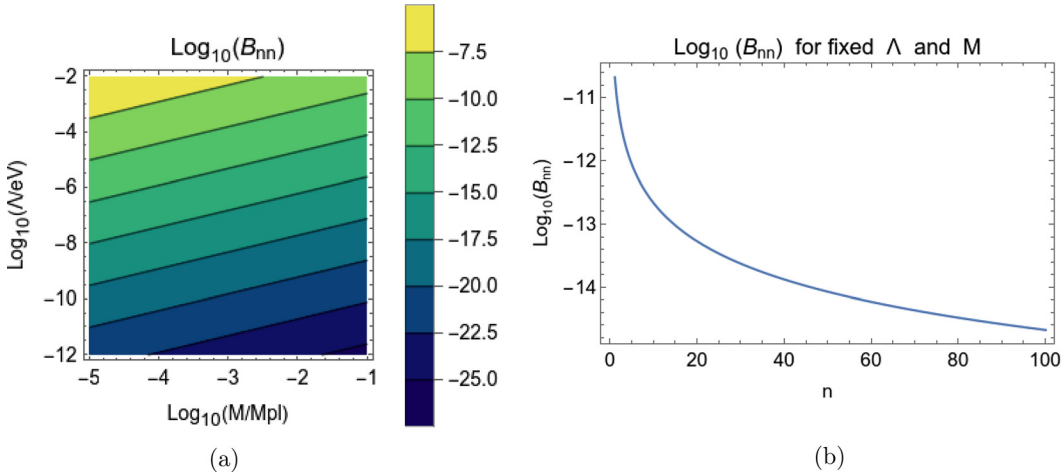

(a) (b)

FIG. 1. Plots of the logarithmic values of the chameleon contribution to the β-coefficients and the particle number for the chameleon model $N = 1$. (a) shows the contour plot of such a contribution as a function of Λ and M for fixed the quantum number $n = 1$. For this part of the parameter space, $u \gg 1$ is true. Plot (b) shows the contribution as a function of the quantum number n for $\Lambda = 1 \times 10^{-3}$ eV and $M = 1 \times 10^{-1} M_{Pl}$.

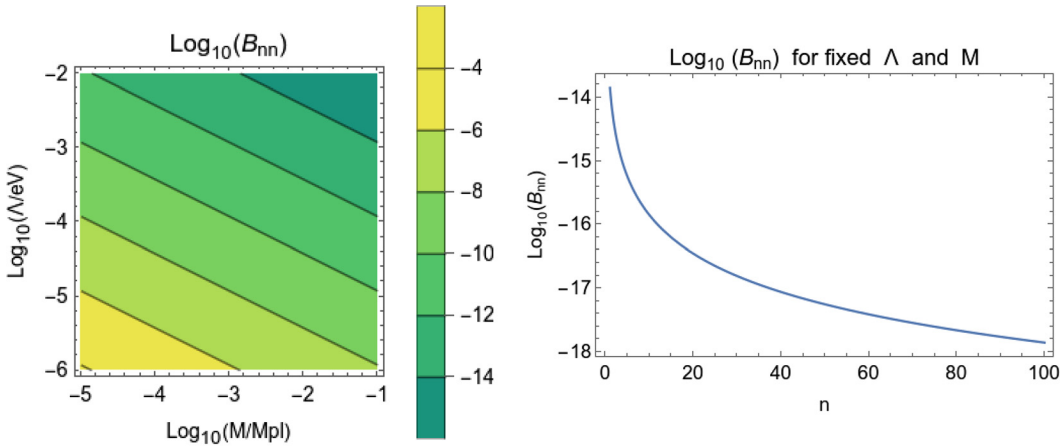

FIG. 2. Plots of the logarithmic values of the chameleon contribution to the β-coefficients and the particle number for the chameleon model $N = -4$. Plot (a) shows the contribution as a function of Λ and M for the fixed quantum number $n = 1$. For this part of the parameter space, $u \gg 1$ is true. Plot (b) shows the contribution as a function of the quantum number n for $\Lambda = 1 \times 10^{-3}$ eV and $M = 1 \times 10^{-1} M_{Pl}$.

This difference in behavior can be understood by examining the chameleon-induced force. The acceleration experienced by a test particle due to a chameleon field near a spherical source mass is given by Ref. 111,

$$\mathbf{a} = -\nabla \ln A(\varphi) = -\frac{\nabla\varphi}{M} = -\frac{R}{Mr^2}(\varphi_{bg} - \varphi_{obj})\mathbf{r}, \qquad (50)$$

where A is the conformal coupling factor defined in Eqs. (1) and (5), and we have used the chameleon field profile in Eq. (7). It can immediately be seen that a smaller M results in a stronger force. When comparing Eqs. (47) and (49), we see that the chameleon field scales oppositely with Λ for $N = 1$ and $N = -4$ models, i.e., φ_{bg} increases with increasing Λ for $N = 1$ but decreases for $N = -4$.

Therefore, we come to the natural conclusion that the chameleon field effect on the cavity particle production is the strongest where the chameleon-induced force is also the strongest. In both considered cases for N, we find a reduction in the particle production of the usual DCE due to the presence of the chameleon scalar field.

IV. CONCLUSIONS

In this paper, we have shown the effect of a chameleon field on the number of particles created in a massive quantum scalar field by the DCE. We have considered an effectively one-dimensional cavity, with one of its boundaries allowed to move, placed near a chameleon source mass. Since the chameleon field is coupled to the mass of the quantum field, the Klein–Gordon equation and, in particular, the Lagrange–Beltrami operator acting on the quantum field in a spatial hypersurface, are affected by the chameleon field. We then computed the Bogoliubov coefficients in the presence of parametric resonances using the techniques developed in Ref. 25. For this computation, we have linearized the chameleon field profile, in analogy to studies of linearizations of the Newtonian potential.[20] As expected, when the chameleon is turned off, the Bogoliubov coefficients are those of the DCE in Minkowski spacetime. Finally, we have analyzed how the particle content is affected by the presence of the chameleon field. We showed that the mean number of created particles is diminished by the presence of the chameleon field, and we gave representative numerical estimates for how the particle content is affected depending on the choice of the chameleon model, the parameters of the model, and the mode number of the quantum field.

This work can also be seen as an extension of the method presented in Refs. 24 and 25 since, for the first time, we were effectively considering a spatially dependent mass, which we can define as $\tilde{m}_\Phi(x) := A^2(\varphi(x))m_\Phi$. We note that the results presented here are constructed with a toy model in the absence of gravity, i.e., no gravitational effect due to the source mass generating the chameleon field gradient. Any testable predictions will need to include a more realistic and sophisticated model, which will most likely only be solvable numerically.

To our knowledge, this article is the first work on the effect of screened scalar fields on particle creation. In the future, it will be interesting to create a more realistic study, also taking into account the gravitational field, not linearizing the chameleon field, and treating the chameleon as a quantum field as in Refs. 90–93. The last would lead to loop corrections that could potentially be significant for the DCE, cp. Refs. 112–116. However, such a fully quantum treatment is beyond the scope of the present article. In addition, other screened scalar field models could also be studied in the same way, and we leave for future work the study of entanglement between modes, their relation to the chameleon parameters, and the implementation of quantum metrology to estimate and constrain chameleon parameters.

ACKNOWLEDGMENTS

The authors are grateful to Luis C. Barbado, Tupac Bravo, Jesús DelOlmo-Márquez, Dennis Rätzel, Dmitrii Trunin, and Jan Kohlrus for useful discussions. A.L.B.-C. recognizes support from CONAHCyT ref:579920/410674. This research was funded in whole or in part by the Austrian Science Fund (FWF) (10.55776/P34240 and 10.55776/PAT8564023) and is based upon work from COST Action COSMIC WISPers CA21106, supported by COST (European Cooperation in Science and Technology). For open access purposes,

AUTHOR DECLARATIONS

Conflict of Interest

The authors have no conflicts to disclose.

Author Contributions

Ana Lucia Báez-Camargo: Conceptualization (equal); Data curation (supporting); Formal analysis (lead); Funding acquisition (equal); Investigation (lead); Methodology (equal); Software (equal); Visualization (equal); Writing – original draft (lead); Writing – review & editing (supporting). **Daniel Hartley:** Conceptualization (supporting); Data curation (equal); Formal analysis (equal); Investigation (equal); Methodology (supporting); Software (lead); Validation (equal); Visualization (equal); Writing – original draft (equal); Writing – review & editing (equal). **Christian Käding:** Conceptualization (supporting); Data curation (lead); Formal analysis (equal); Funding acquisition (equal); Investigation (equal); Methodology (supporting); Software (supporting); Validation (equal); Visualization (equal); Writing – original draft (equal); Writing – review & editing (equal). **Ivette Fuentes-Guridi:** Conceptualization (equal); Formal analysis (supporting); Funding acquisition (equal); Investigation (supporting); Methodology (equal); Supervision (lead); Validation (equal); Visualization (equal); Writing – review & editing (lead).

DATA AVAILABILITY

The data that support the findings of this study are available within the article.

APPENDIX: DERIVATION OF THE NORMALIZATION CONSTANT

In order to compute the normalization constant in Eq. (39), we use Eq. (34) and another linearization of $u^{-1/2}(x)$ at the point s. Thus, the integral of the constant in Eq. (39) is

$$\begin{aligned} I &= \int_{x_l}^{x_r} \mathrm{d}x\, u^{-1/2}(x) \sin^2\left(\frac{2}{3}u^{3/2}(x) - \frac{2}{3}u^{3/2}(x_l)\right) \\ &= \int_{x_l}^{x_r} \mathrm{d}x \left([u(s)]^{-1/2}\left(1 - \frac{1}{2}[u(s)]^{-1}u'(s)(x-s)\right)\right) \\ &\quad \cdot \sin^2\left(\frac{2}{3}[u(s)]^{1/2}\left[\frac{3}{2}u'(s)x - \frac{3}{2}u'(s)x_l\right]\right). \end{aligned} \tag{A1}$$

Hence,

$$\begin{aligned} I &= [u(s)]^{-1/2}\left\{\frac{(x-s)}{2}\left(1 + \frac{1}{2}su^{-1}(s)u'(s)\right)\right. \\ &\quad \left. -\frac{1}{2}u^{-1}(s)u'(s)\left(\frac{(x^2-s^2)}{4}\right)\right\}_{x_l}^{x_r} \\ &= [u(s)]^{-1/2}\frac{L}{2}\left\{1 + \left(\frac{s}{2} - \frac{2s+L}{4}\right)u^{-1}(s)u'(s)\right\}. \end{aligned} \tag{A2}$$

Substituting Eq. (29) in Eq. (A2), we obtain

$$\begin{aligned} I &= \left[\left(\frac{\lambda_n^2}{a} - s\right)(a)^{1/3}\right]^{-1/2}\frac{L}{2}\left\{1 + \left(\frac{s}{2} - \frac{2s+L}{4}\right)[u(s)]^{-1}u'(s)\right\} \\ &= \frac{(a)^{1/2}}{\left[\lambda_n^2 - as\right]^{1/2}(a)^{1/6}}\frac{L}{2}\left\{1 + \frac{L}{4}\left(\frac{a}{(\lambda_n^2 - as)}\right)\right\}. \end{aligned} \tag{A3}$$

Replacing Eq. (A3) in Eq. (39), we have that

$$\mathcal{A}_n = \left[2\omega_n^0\frac{(a)^{1/3}}{\left[\lambda_n^2 - as\right]^{1/2}}\frac{L}{2}\left\{1 + \frac{L}{4}\left(\frac{a}{(\lambda_n^2 - as)}\right)\right\}\right]^{-1/2}. \tag{A4}$$

Plugging Eq. (28) into Eq. (A4), we finally obtain Eq. (40).

REFERENCES

[1] N. D. Birrell and P. C. W. Davies, *Quantum Fields in Curved Space*, Cambridge Monographs on Mathematical Physics (Cambridge University Press, Cambridge, UK, 1984).
[2] R. M. Wald, *Quantum Field Theory in Curved Space-Time and Black Hole Thermodynamics*, Chicago Lectures in Physics (University of Chicago Press, Chicago, IL, 1995).
[3] L. E. Parker and D. Toms, *Quantum Field Theory in Curved Spacetime: Quantized Field and Gravity*, Cambridge Monographs on Mathematical Physics (Cambridge University Press, 2009).
[4] L. Parker, Phys. Rev. Lett. **21**, 562 (1968).
[5] L. Parker, Phys. Rev. **183**, 1057 (1969).
[6] S. W. Hawking, Commun. Math. Phys. **43**, 199 (1975); **46**, 206(E) (1976).
[7] W. G. Unruh, Phys. Rev. D **14**, 870 (1976).
[8] G. T. Moore, J. Math. Phys. **11**, 2679 (1970).
[9] V. V. Dodonov, J. Phys.: Conf. Ser. **161**, 012027 (2009).
[10] B. A. Juárez-Aubry and R. Weder, Rev. Mex. Fis. Suppl. **3**, 020714 (2022).
[11] V. V. Dodonov, MDPI Phys. **2**, 67 (2020).
[12] S. A. Fulling and P. C. W. Davies, Proc. R. Soc. London, Ser. A **348**, 393 (1976).
[13] D. A. R. Dalvit, F. D. Mazzitelli, and X. O. Millan, J. Phys. A **39**, 6261 (2006).
[14] F. Pascoal, L. C. Céleri, S. S. Mizrahi, and M. H. Y. Moussa, Phys. Rev. A **78**, 032521 (2008).
[15] W. Naylor, Phys. Rev. A **86**, 023842 (2012).
[16] N. Friis and I. Fuentes, J. Mod. Opt. **60**, 22 (2013).
[17] X. Busch, R. Parentani, and S. Robertson, Phys. Rev. A **89**, 063606 (2014).
[18] S. Felicetti, M. Sanz, L. Lamata, G. Romero, G. Johansson, P. Delsing, and E. Solano, Phys. Rev. Lett. **113**, 093602 (2014).
[19] I. Romualdo, L. Hackl, and N. Yokomizo, Phys. Rev. D **100**, 065022 (2019).
[20] L. C. Céleri, F. Pascoal, and M. H. Y. Moussa, Classical Quantum Gravity **26**, 105014 (2009).
[21] M. P. E. Lock and I. Fuentes, New J. Phys. **19**, 073005 (2017).
[22] B. A. Juárez-Aubry and R. Weder, "Quantum field theory with dynamical boundary conditions and the Casimir effect," in *Theoretical Physics, Wavelets, Analysis, Genomics: An Indisciplinary Tribute to Alex Grossmann* (Springer International Publishing, Cham, Switzerland, 2023), pp. 195–238.
[23] B. A. Juárez-Aubry and R. Weder, J. Phys. A **54**, 105203 (2021).
[24] L. C. Barbado, A. L. Báez-Camargo, and I. Fuentes, Eur. Phys. J. C **80**, 796 (2020).
[25] L. C. Barbado, A. L. Báez-Camargo, and I. Fuentes, Eur. Phys. J. C **81**, 953 (2021).
[26] R. M. Wald, *General Relativity* (Chicago University Press, Chicago, 1984).
[27] Y. Choquet-Bruhat, *Introduction to General Relativity, Black Holes and Cosmology* (Oxford University Press, 2023).
[28] B. P. Abbott *et al.*, Phys. Rev. Lett. **116**, 061102 (2016).
[29] Y. Fujii and K.-i. Maeda, *The Scalar-Tensor Theory of Gravitation*, Cambridge Monographs on Mathematical Physics (Cambridge University Press, 2003).

[30]V. I. Borodulin, R. N. Rogalyov, and S. R. Slabospitskii, arXiv:1702.08246 (2017).
[31]M. Battaglieri *et al.*, arXiv:1707.04591 (2017).
[32]P. W. Higgs, Phys. Lett. **12**, 132 (1964).
[33]P. W. Higgs, Phys. Rev. Lett. **13**, 508 (1964).
[34]G. Aad *et al.*, Phys. Lett. B **716**, 1 (2012).
[35]T. Clifton, P. G. Ferreira, A. Padilla, and C. Skordis, Phys. Rep. **513**, 1 (2012).
[36]A. Joyce, B. Jain, J. Khoury, and M. Trodden, Phys. Rep. **568**, 1 (2015).
[37]J. O. Dickey *et al.*, Science **265**, 482 (1994).
[38]E. G. Adelberger, B. R. Heckel, A. E. Nelson, and R. Ann, Nucl. Part. Sci. **53**, 77 (2003).
[39]D. J. Kapner, T. S. Cook, E. G. Adelberger, J. H. Gundlach, B. R. Heckel, C. D. Hoyle, and H. E. Swanson, Phys. Rev. Lett. **98**, 021101 (2007).
[40]C. Burrage and J. Sakstein, Living Rev. Rel. **21**, 1 (2018).
[41]J. Khoury and A. Weltman, Phys. Rev. D **69**, 044026 (2004).
[42]J. Khoury and A. Weltman, Phys. Rev. Lett. **93**, 171104 (2004).
[43]H. Dehnen, H. Frommert, and F. Ghaboussi, Int. J. Theor. Phys. **31**, 109 (1992).
[44]E. Gessner, Astrophys. Space Sci. **196**, 29 (1992).
[45]T. Damour and A. M. Polyakov, Nucl. Phys. B **423**, 532 (1994).
[46]M. Pietroni, Phys. Rev. D **72**, 043535 (2005).
[47]K. A. Olive and M. Pospelov, Phys. Rev. D **77**, 043524 (2008).
[48]P. Brax, C. van de Bruck, A.-C. Davis, and D. Shaw, Phys. Rev. D **82**, 063519 (2010).
[49]K. Hinterbichler and J. Khoury, Phys. Rev. Lett. **104**, 231301 (2010).
[50]K. Hinterbichler, J. Khoury, A. Levy, and A. Matas, Phys. Rev. D **84**, 103521 (2011).
[51]C. Burrage, E. J. Copeland, and P. Millington, Phys. Rev. D **95**, 064050 (2017); **95**, 129902 (2017).
[52]C. A. J. O'Hare and C. Burrage, Phys. Rev. D **98**, 064019 (2018).
[53]C. Burrage, E. J. Copeland, C. Käding, and P. Millington, Phys. Rev. D **99**, 043539 (2019).
[54]C. Käding, Astronomy **2**, 128 (2023).
[55]G. R. Dvali, G. Gabadadze, and M. Porrati, Phys. Lett. B **485**, 208 (2000).
[56]A. Nicolis, R. Rattazzi, and E. Trincherini, Phys. Rev. D **79**, 064036 (2009).
[57]A. Ali, R. Gannouji, M. W. Hossain, and M. Sami, Phys. Lett. B **718**, 5 (2012).
[58]M. Gasperini, F. Piazza, and G. Veneziano, Phys. Rev. D **65**, 023508 (2002).
[59]T. Damour, F. Piazza, and G. Veneziano, Phys. Rev. D **66**, 046007 (2002).
[60]T. Damour, F. Piazza, and G. Veneziano, Phys. Rev. Lett. **89**, 081601 (2002).
[61]P. Brax, C. van de Bruck, A.-C. Davis, B. Li, and D. J. Shaw, Phys. Rev. D **83**, 104026 (2011).
[62]P. Brax, H. Fischer, C. Käding, and M. Pitschmann, Eur. Phys. J. C **82**, 934 (2022).
[63]C. Burrage and J. Sakstein, J. Cosmol. Astropart. Phys. **11**, 045 (2016).
[64]Y. N. Pokotilovski, Phys. Lett. B **719**, 341 (2013).
[65]Y. N. Pokotilovski, J. Exp. Theor. Phys. **116**, 609 (2013); **116**, 886 (2013).
[66]T. Jenke *et al.*, Phys. Rev. Lett. **112**, 151105 (2014).
[67]C. Burrage, E. J. Copeland, and E. A. Hinds, J. Cosmol. Astropart. Phys. **3**, 042 (2015).
[68]P. Hamilton, M. Jaffe, P. Haslinger, Q. Simmons, H. Müller, and J. Khoury, Science **349**, 849 (2015).
[69]H. Lemmel, P. Brax, A. N. Ivanov, T. Jenke, G. Pignol, M. Pitschmann, T. Potocar, M. Wellenzohn, M. Zawisky, and H. Abele, Phys. Lett. B **743**, 310 (2015).
[70]C. Burrage and E. J. Copeland, Contemp. Phys. **57**, 164 (2016).
[71]B. Elder, J. Khoury, P. Haslinger, M. Jaffe, H. Müller, and P. Hamilton, Phys. Rev. D **94**, 044051 (2016).
[72]A. N. Ivanov, G. Cronenberg, R. Höllwieser, M. Pitschmann, T. Jenke, M. Wellenzohn, and H. Abele, Phys. Rev. D **94**, 085005 (2016).
[73]C. Burrage, A. Kuribayashi-Coleman, J. Stevenson, and B. Thrussell, J. Cosmol. Astropart. Phys. **12**, 041 (2016).
[74]M. Jaffe, P. Haslinger, V. Xu, P. Hamilton, A. Upadhye, B. Elder, J. Khoury, and H. Müller, Nat. Phys. **13**, 938 (2017).
[75]P. Brax and M. Pitschmann, Phys. Rev. D **97**, 064015 (2018).
[76]D. O. Sabulsky, I. Dutta, E. A. Hinds, B. Elder, C. Burrage, and E. J. Copeland, Phys. Rev. Lett. **123**, 061102 (2019).
[77]P. Brax, C. Burrage, and A.-C. Davis, Int. J. Mod. Phys. D **27**, 1848009 (2018).
[78]G. Cronenberg, P. Brax, H. Filter, P. Geltenbort, T. Jenke, G. Pignol, M. Pitschmann, M. Thalhammer, and H. Abele, Nat. Phys. **14**, 1022 (2018).
[79]T. Jenke, J. Bosina, J. Micko, M. Pitschmann, R. Sedmik, and H. Abele, Eur. Phys. J. Spec. Top. **230**, 1131 (2021).
[80]M. Pitschmann, Phys. Rev. D **103**, 084013 (2021); **106**, 109902 (2022).
[81]S. Qvarfort, D. Rätzel, and S. Stopyra, New J. Phys. **24**, 033009 (2022).
[82]P. Brax, S. Casas, H. Desmond, and B. Elder, Universe **8**, 11 (2021).
[83]P. Yin, R. Li, C. Yin, X. Xu, X. Bian, H. Xie, C.-K. Duan, P. Huang, J.-h. He *et al.*, Nat. Phys. **18**, 1181 (2022).
[84]J. Betz, J. Manley, E. M. Wright, D. Grin, and S. Singh, Phys. Rev. Lett. **129**, 131302 (2022).
[85]D. Hartley, C. Käding, R. Howl, and I. Fuentes, Eur. Phys. J. C **84**, 49 (2024).
[86]H. Fischer, C. Käding, R. I. P. Sedmik, H. Abele, P. Brax, and M. Pitschmann, Phys. Dark Universe **43**, 101419 (2024).
[87]H. Fischer, C. Käding, H. Lemmel, S. Sponar, and M. Pitschmann, Prog. Theor. Exp. Phys. **2024**, 023E02.
[88]H. Fischer and R. I. P. Sedmik, arXiv:2401.16179 (2024).
[89]G. L. Klimchitskaya and V. M. Mostepanenko, Universe **10**(3), 119 (2024).
[90]P. Brax and S. Fichet, Phys. Rev. D **99**, 104049 (2019).
[91]C. Burrage, C. Käding, P. Millington, and J. Minář, Phys. Rev. D **100**, 076003 (2019).
[92]C. Burrage, C. Käding, P. Millington, and J. Minář, J. Phys.: Conf. Ser. **1275**, 012041 (2019).
[93]C. Käding, M. Pitschmann, and C. Voith, Eur. Phys. J. C **83**, 767 (2023).
[94]D. Hartley, C. Käding, R. Howl, and I. Fuentes, Phys. Rev. D **99**, 105002 (2019).
[95]Recently, a proposal has been made to use Casimir experiments to constrain symmetron models.[117] However, in this article, we will only consider chameleon fields and leave symmetrons to future investigation.
[96]D. F. Mota and D. J. Shaw, Phys. Rev. D **75**, 063501 (2007).
[97]P. Brax, C. van de Bruck, A.-C. Davis, D. F. Mota, and D. J. Shaw, Phys. Rev. D **76**, 124034 (2007).
[98]P. Brax, C. van de Bruck, A. C. Davis, D. J. Shaw, and D. Iannuzzi, Phys. Rev. Lett. **104**, 241101 (2010).
[99]P. Brax and A.-C. Davis, Phys. Rev. D **91**, 063503 (2015).
[100]A. Almasi, P. Brax, D. Iannuzzi, and R. I. P. Sedmik, Phys. Rev. D **91**, 102002 (2015).
[101]P. Brax, A.-C. Davis, and B. Elder, Phys. Rev. D **107**, 084025 (2023).
[102]H. Haghmoradi, H. Fischer, A. Bertolini, I. Galić, F. Intravaia, M. Pitschmann, R. Schimpl, and R. I. P. Sedmik, arXiv:2403.10998 (2024).
[103]A more general class of scalar-tensor field models can be constructed from the disformal transformation $g'_{\mu\nu} = A^2(\varphi)g_{\mu\nu} + B(\varphi)\partial_\mu\varphi\partial_\nu\varphi$.[118] For an overview of disformally coupled scalar field models, see Ref. 119.
[104]While the physical equivalence of Einstein and Jordan frames is often considered, it is still a subject to debate whether it also holds at the quantum level,[120–122] and it was shown that, in the Hamiltonian formalism, a conformal transformation is not canonical.[123] However, in this article, we work in a classical background.
[105]There are some authors that compute the DCE in three dimensions.[20,124,125] We consider the one-dimensional case because the transverse momentum does not appear, which simplifies the calculations. Moreover, experimental investigations of the DCE primarily work in one dimension.[126–128]
[106]The reduction from a three spatial dimensional problem is done by assuming that two cavity dimensions are much smaller than the third one, such that the system can be effectively treated in one spatial dimension. This is due to the direction of the chameleon field gradient being radial, and therefore no significant effects occurring in the transverse directions.
[107]F. Sorge, Classical Quantum Gravity **22**, 5109 (2005).
[108]J.-Y. Ji, H.-H. Jung, J.-W. Park, and K.-S. Soh, Phys. Rev. A **56**, 4440 (1997).
[109]C. Sabín, D. E. Bruschi, M. Ahmadi, and I. Fuentes, New J. Phys. **16**, 085003 (2014).
[110]With the parameters of Table I, all the approximations made in this work are fulfilled, namely, $\varphi/M \ll 1$ and $\varepsilon L \ll L \ll s \ll R_{vac} \ll m_{bg}^{-1}$.
[111]J. Khoury, Classical Quantum Gravity **30**, 214004 (2013).
[112]D. A. Trunin, Phys. Rev. D **104**, 045001 (2021).
[113]D. A. Trunin, Eur. Phys. J. C **82**, 440 (2022).

[114]D. A. Trunin, Phys. Rev. D **107**, 065004 (2023).
[115]L. A. Akopyan and D. A. Trunin, Phys. Rev. D **103**, 065005 (2021).
[116]E. T. Akhmedov and S. O. Alexeev, Phys. Rev. D **96**, 065001 (2017).
[117]B. Elder, V. Vardanyan, Y. Akrami, P. Brax, A.-C. Davis, and R. S. Decca, Phys. Rev. D **101**, 064065 (2020).
[118]J. D. Bekenstein, Phys. Rev. D **48**, 3641 (1993).
[119]J. Sakstein, J. Cosmol. Astropart. Phys. **2014**, 012.
[120]V. Faraoni and S. Nadeau, Phys. Rev. D **75**, 023501 (2007).
[121]N. Banerjee and B. Majumder, Phys. Lett. B **754**, 129 (2016).
[122]S. Pandey and N. Banerjee, Eur. Phys. J. Plus **132**, 107 (2017).
[123]S. J. Gabriele Gionti, Phys. Rev. D **103**, 024022 (2021).
[124]I. Bialynicki-Birula and Z. Bialynicka-Birula, Phys. Rev. A **78**, 042109 (2008).
[125]E. Sassaroli, Y. N. Srivastava, J. Swain, and A. Widom, arXiv:hep-ph/9805479 (1998).
[126]C. M. Wilson, G. Johansson, A. Pourkabirian, M. Simoen, J. R. Johansson, T. Duty, F. Nori, and P. Delsing, Nature **479**, 376 (2011).
[127]P. Lähteenmäki, G. S. Paraoanu, J. Hassel, and P. J. Hakonen, Proc. Natl. Acad. Sci. **110**, 4234 (2013).
[128]I.-M. Svensson, M. Pierre, M. Simoen, W. Wustmann, P. Krantz, A. Bengtsson, G. Johansson, J. Bylander, V. Shumeiko *et al.*, J. Phys.: Conf. Ser. **969**, 012146 (2018).